Enzyme-Based Impedimetric Biosensor dotted with gold nanoparticles

Zuzana Košelová
Department of Microelectronics
Faculty of Electrical Engineering and Communication,
Brno University of Technology,
Brno, 612 00, Czech Republic
225675@vut.cz

Zdenka Fohlerová
Department of Microelectronics
Faculty of Electrical Engineering and Communication
Brno University of Technology
Brno, 612 00, Czech Republic
fohlerova@vutbr.cz

***Abstract*— This research delves into the realm of biosensor improvement through the utilization of gold nanoparticles (Au NPs). The primary objective is to assess the impact of different-sized Au NPs on sensor performance, specifically investigating whether 100 nm or 20 nm nanoparticles prove more favourable to enhancement. Moreover, we aim to inspect the biosensor's response to varied concentrations of Au NPs, unravelling the involved collaboration between nanoparticle size, concentration, and overall sensor properties. This modification of commercial electrodes with Au NPs, could be way for enhancing surface area and enzyme immobilization. Notably, the investigation also explores the potential drawbacks associated with increasing nanoparticle concentration and offers insights into optimizing biosensor design. It has been observed that while 20 nm Au NPs slightly decreased impedance values at higher glucose concentrations, 100 nm Au NPs, conversely, exhibited an increase in capacitive behaviour. Equally crucial is the parameter chosen for constructing the calibration curve. From impedance values at low frequencies of alternating voltage, such as 2 Hz, a lower Limit of Detection (LOD) is obtained. However, the analysis of R_{ct} in the case of 20 nm Au NPs reveals a broader range of glucose concentrations falling within the calibration area. Through a comprehensive analysis of electrochemical behaviour, impedance, and charge transfer resistance, we endeavour to provide contributions to the improvement of biosensor technologies.**

Keywords—gold nanoparticles, biosensors, enzyme immobilization, impedance spectroscopy, glucose detection, calibration curves

I. INTRODUCTION

Over the past decade, there has been a growing interest in the modification of sensors using nanomaterials, offering advantages such as increased surface area, enhanced restriction, and improved selectivity. These modifications prove beneficial for applications like third-generation sequencing and direct detection events involving affinity partners, such as DNA hybridization or antigen-antibody interactions [1]. Various techniques are employed for creating nanoscale structures, ranging from sophisticated methods like ion beam etching to simpler approaches like anodization [2][3]. Among these methods, the packing of spherical nanoparticles (NPs) in a dense planar arrangement has gained attention [4][5]. By precisely choosing the material and shape of NPs, a versatile system suitable for a wide range of applications can be produced. In this study, we explore and tests a strategy to enhance the Limit of Detection (LOD) in biosensors, focusing on enlarging the surface area for enzyme storage. The idea is that a densely covered surface by enzyme will reach saturation later. Expanding the electrode surface with NPs provides more space for immobilization while using the same electrodes, allowing us to test whether this approach increases sensitivity. Even though gold nanoparticles (Au NPs) are primarily utilized in optical biosensors, the widespread use in enzyme-based biosensors is notable [6][7][8]. Au NPs exhibit high conductivity and biocompatibility, potentially able forming strong bonds with organic substances (with enhancement of the right chemical groups). This unique feature creates a suitable microenvironment for enzyme immobilization, significantly enhancing enzyme activity [9]. Enzymes, owing to their numerous functional groups such as carboxylic (–COOH), amino (–NH2), thiol (–SH), etc., can be easily immobilized directly onto nanoparticles [9]. There are numerous combinations in which these nanoparticles have been incorporated into biosensing. However, they are mostly used in their oxidized form, as ions, as it makes them more easily electrochemically detectable. For example, Ilkhani et al. [10] also utilized citrate doped Au NPs, although with a differential pulse voltammetry setup (particle diameter = 32 nm, concentration = 0.268 μg/mL, LOD = 50 pg/mL). Additionally, Au NPs on gold electrodes have also been tested primarily using amperometry (particle diameter = 11 nm, LOD = 23 μM) [11], (particle diameter = 3.4 nm, LOD = 0.5 μM) [12], (particle diameter = 2.6 nm, LOD = 8.2 μM) [13]. However, we are the first to employ AuNPs in a biamperometric setup for calibration measurements using impedance spectroscopy. It is intriguing to note that the addition of nanoparticles has sometimes led to a decrease in biosensor response. According to the authors, this phenomenon may be attributed to the difference in oxidative states between Au NPs and the active centre of the enzyme, as observed in previous studies (colloid containing AuNPs at 5,5 mM) [14]. In our investigation, we aim to scrutinize the effectiveness of sensor enhancement through the utilization of both larger and smaller Au nanoparticles (NPs). The central focus is to discern how the biosensor will respond to varying concentrations of these NPs, evaluating whether their presence will predominantly favour the overall performance or potentially exhibit contrasting effects. By delving into this exploration, we seek to unravel insights that can contribute to refining the design and application of biosensors, particularly those utilizing Au NPs for surface modification.

II. Methods and Materials

A. Chemicals

Gold nanoparticles (Au NPs) of diameter 20 and 100 nm stabilized suspension in citrate buffer, poly-L-lysine hydrobromide (p-lys), glucose oxidase (GOD) from Aspergillus Niger, bovine serum albumin (BSA), Hexaammineruthenium(III) chloride (98%) (Ru3+), potassium ferrocyanide and potassium ferricyanide (Fe2+/Fe3+), glutaraldehyde solution (GO) (25%), were purchased from Sigma-Aldrich (Germany). D-(+)-Glucose monohydrate, KOH, H_2O_2 (30%), isopropyl alcohol was purchased from Penta (Czech Republic).

B. Electrodes

In this study, commercial electrodes from a biamperometric setup (www.printed.cz, Czech Republic) consisting of a pair of two identical gold disk electrodes were utilized. These electrodes have an internal diameter of 400 µm and lack a separate reference or counter electrode. The immobilization of gold nanoparticles (Au NPs) with diameters ≈ 20 nm and concentration 6.54 10^{11} particles/mL, as well as ≈ 100 nm with concentration 3.8 10^{9} particles/mL was carried out on a positively charged poly-L-lysine (p-lys) thin layer.

Before modifying the electrodes, an "activation" process was performed on the gold electrodes. The electrodes underwent polishing with microcloth (Buehler) and isopropyl alcohol to eliminate residual photoresist and passivation layers from the surface. Subsequently, the electrodes were treated with a solution of 0.5 M KOH and 20% H_2O_2 for 10 min. To functionalize the gold electrode, a 50 µg/mL p-lysine in phosphate-buffered saline (PBS; 10 mM, pH 7.4) was adsorbed onto the electrode surface for at least 30 minutes, providing amino groups on the gold surface. Following washing and drying steps, a drop of negatively charged Au NPs solution was applied to the positively charged modified electrode for 40 minutes.

The mixture of 16 µl GOD (8 mg/ml) and 25 µl BSA (16 mg/ml) was then cross-linked with 2.75 µl 2% glutaraldehyde solution (GO). All were dissolved in PBS (10 mM; pH 7.3). This microliter mixture was applied to the Au NPs-modified electrodes and allowed to dry. The reference sample without GOD was created with 33 µl BSA (13 mg/ml) and 2.75 µl of a 2% glutaraldehyde solution. Additionally, a reference without NPs was created by cross-linking the GOD enzyme with BSA on p-lysine.

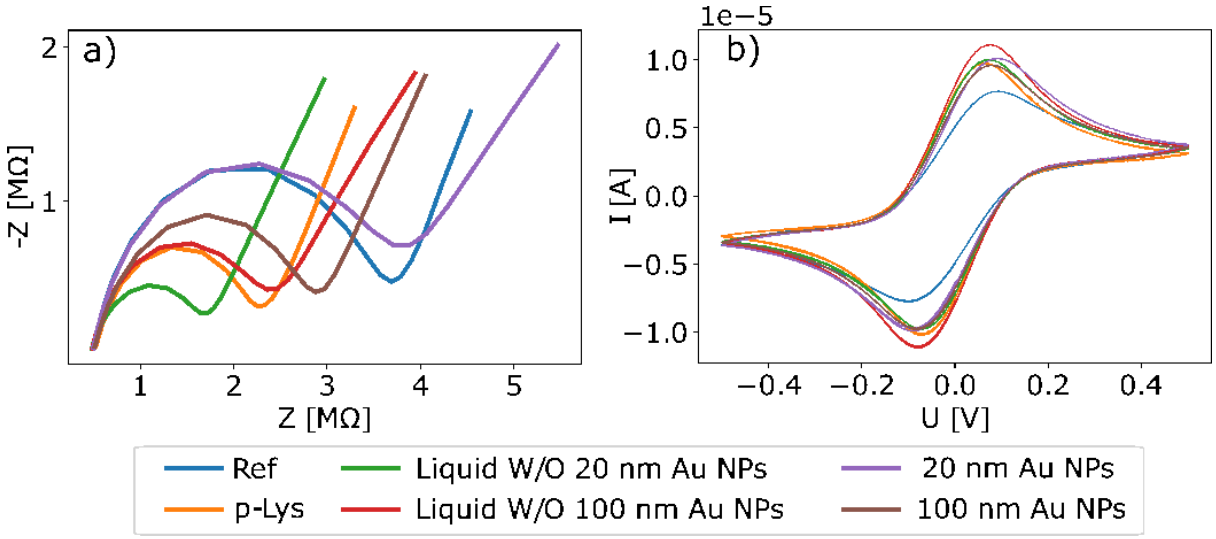

Fig. 1. Graph presents Nyquist plot (a) and CV (b) for the electrodes after modification steps observed in the presence of the Fe2+/Fe3+ redox probe. Citrat20 and Citrat100 represent the liquid without NPs, serving as reference points to elucidate electrode reactions unaffected by the influence of gold nanoparticles (Au NPs). And samples labelled Au20 and Au100 are electrodes modified with 20 nm Au NPs and 100 nm Au NPs, respectively.

Electrochemical impedance spectra (EIS) and cyclic voltammetry (CV) were recorded using the µAUTOLAB III / FRA2 (Metrohm Autolab, Netherlands) analyser. For EIS enzymatic measurements, the electrode was placed in a beaker with 2 ml of 5 mM $[Ru(NH_3)_6]_3$ dissolved in PBS. A potential with an amplitude of 50 mV was applied, with a logarithmic distribution of 20 individual frequencies ranging from 100,000 to 2 Hz. The first two measurements were conducted without glucose, followed by a series of measurements with varying glucose concentrations to establish a calibration curve. Glucose was introduced from a solution made of 0.1 M D-(+)-Glucose monohydrate dissolved in PBS.

CV and EIS for confirmation of the modification layers were performed in 50 mM Fe2+/Fe3+ in 10 mM PBS (7.4 pH) as a redox probe. CV measurements were made in the range of -0.5 to 0.5 V. The cycle was repeated twice for each sample. The scan rate was 0.1 V/s and the step potential was 2.44 mV.

III. Results and Discussions

The initial objective was to confirm the immobilization of Au NPs on the electrodes and its impact on glucose sensing. Impedance spectroscopy and cyclic voltammetry measurements using Fe2+/Fe3+ as a redox probe revealed distinct changes in electrode behavior after modification (Fig. 1). The analysis revealed that the immobilization of P-lysine caused a noticeable decrease in impedance. This phenomenon can be attributed to the presence of amino groups, characterized by a positive

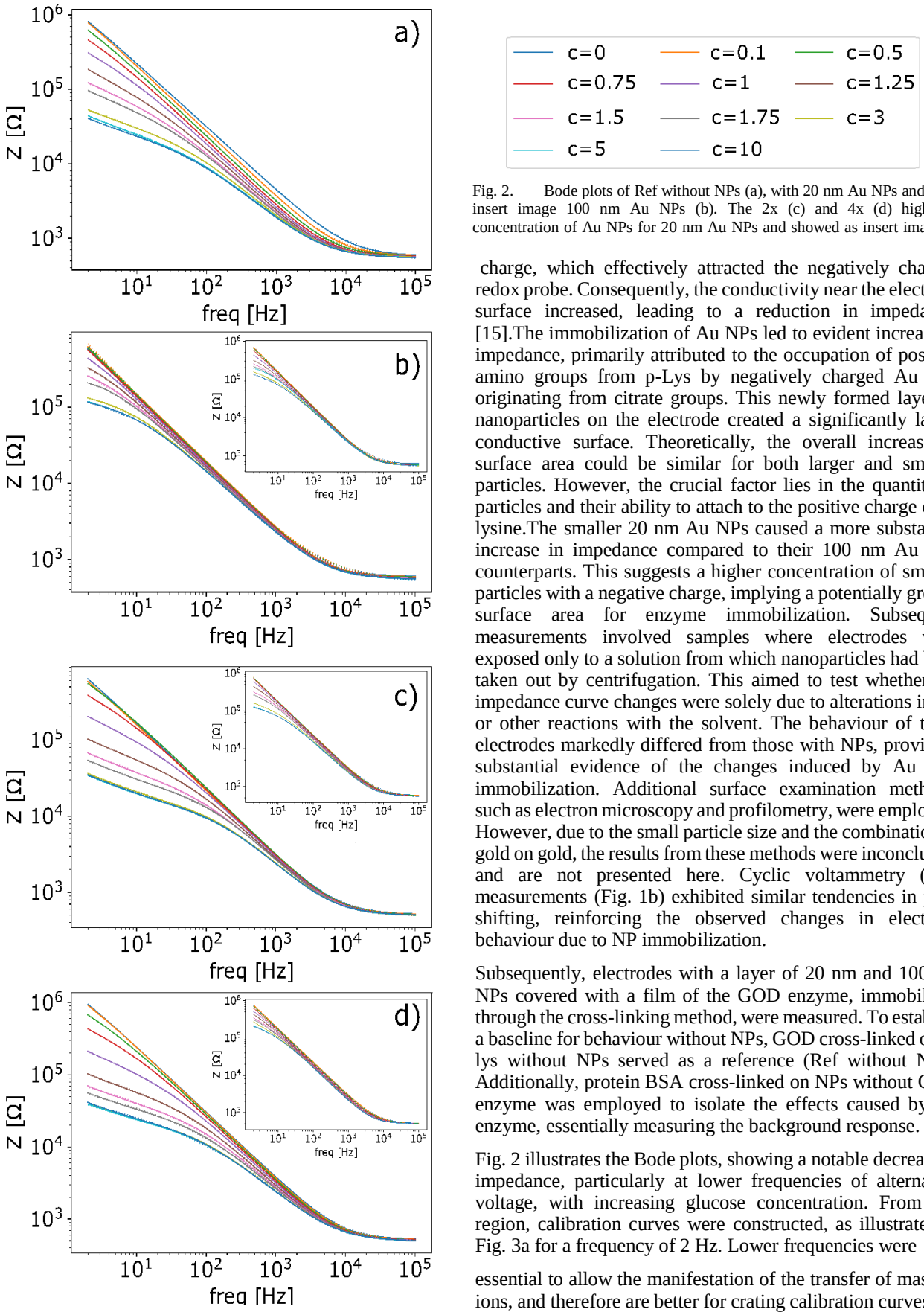

Fig. 2. Bode plots of Ref without NPs (a), with 20 nm Au NPs and as insert image 100 nm Au NPs (b). The 2x (c) and 4x (d) higher concentration of Au NPs for 20 nm Au NPs and showed as insert image

charge, which effectively attracted the negatively charged redox probe. Consequently, the conductivity near the electrode surface increased, leading to a reduction in impedance. [15].The immobilization of Au NPs led to evident increase in impedance, primarily attributed to the occupation of positive amino groups from p-Lys by negatively charged Au NPs originating from citrate groups. This newly formed layer of nanoparticles on the electrode created a significantly larger conductive surface. Theoretically, the overall increase of surface area could be similar for both larger and smaller particles. However, the crucial factor lies in the quantity of particles and their ability to attach to the positive charge of P-lysine.The smaller 20 nm Au NPs caused a more substantial increase in impedance compared to their 100 nm Au NPs counterparts. This suggests a higher concentration of smaller particles with a negative charge, implying a potentially greater surface area for enzyme immobilization. Subsequent measurements involved samples where electrodes were exposed only to a solution from which nanoparticles had been taken out by centrifugation. This aimed to test whether the impedance curve changes were solely due to alterations in pH or other reactions with the solvent. The behaviour of these electrodes markedly differed from those with NPs, providing substantial evidence of the changes induced by Au NPs immobilization. Additional surface examination methods, such as electron microscopy and profilometry, were employed. However, due to the small particle size and the combination of gold on gold, the results from these methods were inconclusive and are not presented here. Cyclic voltammetry (CV) measurements (Fig. 1b) exhibited similar tendencies in peak shifting, reinforcing the observed changes in electrode behaviour due to NP immobilization.

Subsequently, electrodes with a layer of 20 nm and 100 nm NPs covered with a film of the GOD enzyme, immobilized through the cross-linking method, were measured. To establish a baseline for behaviour without NPs, GOD cross-linked on P-lys without NPs served as a reference (Ref without NPs). Additionally, protein BSA cross-linked on NPs without GOD enzyme was employed to isolate the effects caused by the enzyme, essentially measuring the background response.

Fig. 2 illustrates the Bode plots, showing a notable decrease in impedance, particularly at lower frequencies of alternating voltage, with increasing glucose concentration. From this region, calibration curves were constructed, as illustrated in Fig. 3a for a frequency of 2 Hz. Lower frequencies were

essential to allow the manifestation of the transfer of massive ions, and therefore are better for crating calibration curves. To

TABLE I. THIS TABLE SHOWS THE CALIBRATION AREA, PARAMETERS FROM THE CALIBRATION CURVES, AND LOD FOR THE R_{CT} AND IMPEDANCE MEASUREMENTS CONDUCTED AT FREQUENCY 2 HZ. THE VALUES OF R_{CT} HAVE BEEN LOGARITHMICALLY TRANSFORMED TO ACHIEVE LINEAR REPRESENTATION.

Sample	**R_{ct}**			**Z for 2 Hz**			
	Calibration area [mM]	***a [log(Ω).mM^{-1}]***	***LOD [mM]***	***Calibration area [mM]***	***a [MΩ.mM^{-1}]***	***LOD [mM]***	***LOD data er. [mM]***
Ref – no NPs	0.1 – 1.9	-1.22 ± 0.09	0.24	0.01-1.6	-0.50 ± 0.03	0.18	0.10
Au NPs 100	0.5 – 2	-1.2 ± 0.1	0.51	0.1-1.7	-0.35 ± 0.03	0.31	0.14
2x Au NPs 100	0.5 – 1.75	-5.7 ± 1.5	0.89	0.1-2	-0.34 ± 0.06	0.56	0.15
4x Au NPs 100	0.5 – 1.75	-1.4 ± 0.3	0.60	0.1-1.7	-0.32 ± 0.02	0.22	0.15
Au NPs 20	0.5 – 1.75	-4.9 ± 1.7	1.1	0.1-1.8	-0.32 ± 0.03	0.33	0.16
2x Au NPs 20	0.1 – 2	-1.33 ± 0.09	0.23	0.1-1.5	-0.43 ± 0.05	0.42	0.12
4x Au NPs 20	0.1 – 2	-1.3 ± 0.1	0.29	0.01-1.5	-0.66 ± 0.07	0.33	0.08

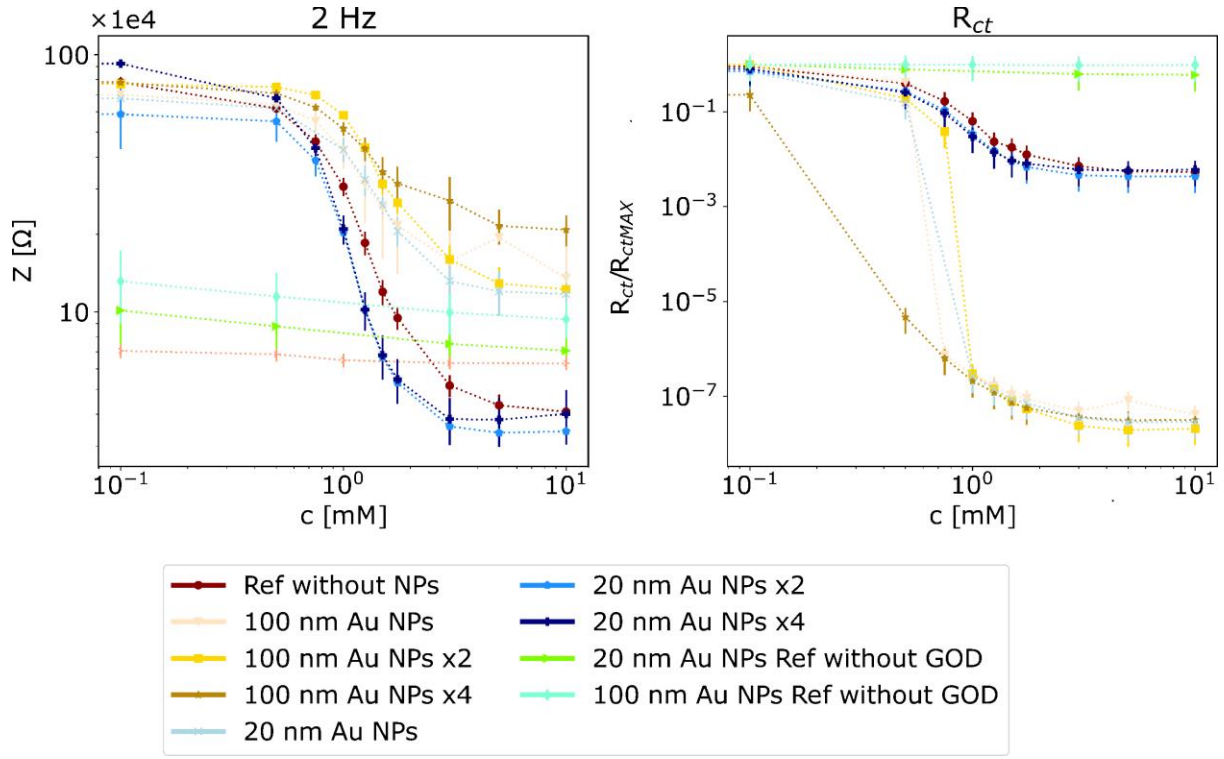

Fig. 3. Graph (a) shows impedance measurement for 2 Hz voltage frequency. Graph (b) shows R_{ct} parameter dependence on glucose concentration. The values were normalized by maximal R_{ct} value for given type of sample. R_{ct} was calculated by fitting Randles equation corresponding to showed circuit (b). 100 nm and 20 nm Au NPs represents diameters and x2/x4 is the multiple of the particle concentration.

further illustrate the electrode behaviour, Nyquist graphs would reveal a gradual formation of more pronounced semicircles with increasing glucose concentrations. For lower concentrations, a distinct diffusional tail would be prominent.

The decline in impedance observed on the electrode surface corresponds to the ongoing reaction. The rise in current is a direct result of the re-oxidation of Ru2+ to Ru3+. Thanks to reaction of glucose oxidation catalysed by glucose oxidase (GOD) the reduction from Ru3+ to Ru2+ is occurring and therefore the free electron can be created for increasement of measured current. To delve deeper into the modifications in electrochemical behaviour, we focused on the charge transfer resistance (R_{ct}). This parameter signifies the difficulty encountered when an electron undergoes transfer from one atom or compound to another (Fig. 3b). The values for R_{ct}, along with their standard deviation (σ_c), were determined through data fitting using the Randles equation. For both 20 nm and 100 nm Au NPs, we conducted measurements with concentrations that the deviations of individual measurements. Reference samples without GOD did not have a calibration curve and were

consequently not included in the table. Generally, regarding our sensors with 20 nm Au NPs, they tended to behave similarly to the reference sample without NPs. In contrast, those with Au NPs exhibited a smaller decrease in impedance but a larger drop in $R_{ct.}$ This suggests that these gold particles might be causing a hindrance rather than accelerating the electron transport to the electrodes. However, since R_{ct} remains low, we can assume that it serves more as a capacitor function rather than a distinct barrier. For practical applications of these biosensors, consideration of the sensor's behaviour is crucial when selecting an appropriate processing form. Ideally, the chosen form should yield an optimal curve and a lower LOD. Generally, calibration from impedance provides a smaller deviation and thus a better LOD, while calibration from R_{ct} can capture a broader concentration range.

IV. Conclusion

It is commonly hypothesized that a larger surface area allows for the immobilization of a greater number of enzymes, potentially enhancing sensitivity. This study investigated this hypothesis using two different-sized Au NPs to monitor their impact on biosensor behaviour. The method of packing spherical NPs in a dense planar arrangement was employed for immobilization, known for its rapid and simple application without the need for sophisticated equipment. It was revealed that the nanoparticle layer significantly influenced the biosensor response in impedance measurement. Larger particles, specifically 100 nm Au NPs, tended to cause blocking, enhancing capacitor behaviour, while 20 nm Au NPs slightly increased electron flow, potentially due to a higher amount of immobilized enzyme available for reaction. However, this effect became noticeable only at an elevated concentration of 20 nm Au NPs. The Limit of Detection (LOD) was lower for calibrations derived from impedance curves. However, we must note that, compared to our reference, the addition of Au NPs rather caused a decrease in LOD, most likely due to further blocking. A decrease in response was also observed in [14]. Further optimization, such different NPs diameter, material or exploring alternative enzyme immobilization techniques, may yield improvements in the calibration range. Continued investigation into the properties of nanopore biosensors could prove valuable, particularly in the development of "point of care" devices.

Acknowledgment

This article was supported by the Czech Academy of Sciences (RVO:68081731) and The Technology Agency of the Czech Republic FW03010504. We acknowledge CzechNanoLab Research Infrastructure supported by The Ministry of Education, Youth and Sports of the Czech Republic (LM2018110), and the project FEKT-S-23-8162 and CEITEC VUT/FEKT-J-24-8567.

References

[1] A. Santos, T. Kumeria, and D. Losic, "Nanoporous anodic aluminum oxide for chemical sensing and biosensors," *TrAC - Trends in Analytical Chemistry*, vol. 44. Elsevier B.V., pp. 25–38, Mar. 01, 2013. doi: 10.1016/j.trac.2012.11.007.

[2] Q. Chen and Z. Liu, "Fabrication and Applications of Solid-State Nanopores," *Sensors*, vol. 19, no. 8, p. 1886, Apr. 2019, doi: 10.3390/s19081886.

[3] S. Manzoor, M. W. Ashraf, S. Tayyaba, and M. K. Hossain, "Recent progress of fabrication, characterization, and applications of anodic aluminum oxide (AAO) membrane: A review," Dec. 2021, Accessed: Mar. 02, 2022. [Online]. Available: http://arxiv.org/abs/2112.08450

[4] J. Sopoušek, J. Věžník, P. Skládal, and K. Lacina, "Blocking the Nanopores in a Layer of Nonconductive Nanoparticles: Dominant Effects Therein and Challenges for Electrochemical Impedimetric Biosensing," *ACS Appl. Mater. Interfaces*, vol. 12, no. 12, pp. 14620–14628, Mar. 2020, doi: 10.1021/acsami.0c02650.

[5] A. de la Escosura-Muñiz, M. Espinoza-Castañeda, M. Hasegawa, L. Philippe, and A. Merkoçi, "Nanoparticles-based nanochannels assembled on a plastic flexible substrate for label-free immunosensing," *Nano Res.*, vol. 8, no. 4, pp. 1180–1188, Apr. 2015, doi: 10.1007/s12274-014-0598-5.

[6] P. Jiang, Y. Wang, L. Zhao, C. Ji, D. Chen, and L. Nie, "Applications of Gold Nanoparticles in Non-Optical Biosensors," *Nanomater. 2018, Vol. 8, Page 977*, vol. 8, no. 12, p. 977, Nov. 2018, doi: 10.3390/NANO8120977.

[7] Z. Hua, T. Yu, D. Liu, and Y. Xianyu, "Recent advances in gold nanoparticles-based biosensors for food safety detection," *Biosens. Bioelectron.*, vol. 179, p. 113076, May 2021, doi: 10.1016/J.BIOS.2021.113076.

[8] C. Shan, H. Yang, D. Han, Q. Zhang, A. Ivaska, and L. Niu, "Graphene/AuNPs/chitosan nanocomposites film for glucose biosensing," *Biosens. Bioelectron.*, vol. 25, no. 5, pp. 1070–1074, Jan. 2010, doi: 10.1016/J.BIOS.2009.09.024.

[9] I. S. Kucherenko, O. O. Soldatkin, D. Y. Kucherenko, O. V. Soldatkina, and S. V. Dzyadevych, "Advances in nanomaterial application in enzyme-based electrochemical biosensors: a review," *Nanoscale Advances*, vol. 1, no. 12. Royal Society of Chemistry, pp. 4560–4577, Dec. 03, 2019. doi: 10.1039/c9na00491b.

[10] H. Ilkhani, M. Sarparast, A. Noori, S. Z. Bathaie, and M. F. Mousavi, "Electrochemical aptamer/antibody based sandwich immunosensor for the detection of EGFR, a cancer biomarker, using gold nanoparticles as a signaling probe," *Biosens. Bioelectron.*, vol. 74, pp. 491–497, Dec. 2015, doi: 10.1016/J.BIOS.2015.06.063.

[11] S. Zhang, N. Wang, Y. Niu, and C. Sun, "Immobilization of glucose oxidase on gold nanoparticles modified Au electrode for the construction of biosensor," *Sensors Actuators B Chem.*, vol. 109, no. 2, pp. 367–374, Sep. 2005, doi: 10.1016/J.SNB.2005.01.003.

[12] T. Zhang, J. Ran, C. Ma, and B. Yang, "A Universal Approach to Enhance Glucose Biosensor Performance by Building Blocks of Au Nanoparticles," *Adv. Mater. Interfaces*, vol. 7, no. 12, p. 2000227, Jun. 2020, doi: 10.1002/ADMI.202000227.

[13] S. Zhang, N. Wang, H. Yu, Y. Niu, and C. Sun, "Covalent attachment of glucose oxidase to an Au electrode modified with gold nanoparticles for use as glucose biosensor," *Bioelectrochemistry*, vol. 67, no. 1, pp. 15–22, Sep. 2005, doi: 10.1016/J.BIOELECHEM.2004.12.002.

[14] G. A. Valencia, L. C. De Oliveira Vercik, and A. Vercik, "A new conductometric biosensor based on horseradish peroxidase immobilized on chitosan and chitosan/gold nanoparticle films," *J. Polym. Eng.*, vol. 34, no. 7, pp. 633–638, Sep. 2014, doi: 10.1515/POLYENG-2014-0072/MACHINEREADABLECITATION/RIS.

[15] K. Lacina, J. Sopoušek, V. Čunderlová, A. Hlaváček, T. Václavek, and V. Lacinová, "Biosensing based on electrochemical impedance spectroscopy: Influence of the often-ignored molecular charge," *Electrochem. commun.*, vol. 93, pp. 183–186, Aug. 2018, doi: 10.1016/j.elecom.2018.07.015.